Interphase Layer Formation in Isotactic Polypropylene/Ethylene–Propylene Rubber Blends

Andrey O. Baranov,[1] Nataliya A. Erina,[1] Sergey A. Kuptsov,[2] Tatiyana I. Medintseva,[1] Eduard V. Prut[1]

[1]*N. N. Semenov's Institute of Chemical Physics, Russian Academy of Sciences, Kosygina 4, Moscow 119991, Russia*
[2]*The Moscow State Pedagogical University, Malaya Pirogovskaya 1, Moscow 119882, Russia*

Received 30 March 2002; accepted 2 September 2002

ABSTRACT: The influence of the interphase layer, formed by the introduction of an oil in ethylene–propylene rubber (EPR), on the structure and properties of isotactic polypropylene (iPP)/EPR blends was studied. The dispersity of the rubber phase in the iPP matrix did not depend on presence of oil. The melting temperature of iPP decreased with increasing content of oil-extended EPR, and it did not change if the oil was absent. The compatibility parameter was determined from the dependency of the iPP melting point on the rubber content with the Nishi–Wang equation. A negative value of the parameter indicated a limited compatibility of iPP with oil-extended EPR. The latter also reduced the temperature and heat of crystallization of iPP. The mechanical properties of iPP/EPR blends were investigated as functions of temperature and elongation rate. It appeared that elastic modulus and yield stress of the blends linearly depended on the logarithm of the elongation rate. Activation volumes, calculated with the Eyring equation, increased with increasing content of elastomer; moreover, this increase was more pronounced for the oil-extended elastomer. It is suggested that the oil influenced the structure of the interphase layer and, accordingly, the characteristics of the iPP/EPR blends. © 2003 Wiley Periodicals, Inc. J Appl Polym Sci 89: 249–257, 2003

Key words: blends; isotactic polypropylene; elastomers; interphase layer; mechanical properties

INTRODUCTION

Isotactic polypropylene (iPP)-based blends represent polymer compositions that have been very actively studied in the last 2 decades.[1,2] As second components in most of these blends, ethylene–propylene rubber (EPR), ethylene–propylene–diene terpolymer (EPDM), butyl and polyisobutylene elastomers, and so on are generally used. At low contents of elastomer, impact-resistant polypropylene is obtained, whereas thermoplastic elastomers are produced at higher elastomer contents. Both classes of materials find wide application that requires detailed consideration of different factors, such as the influence of the chemical and molecular structures of the elastomer, the molecular weight distribution, and so on, of the properties of the finished products.

One important factor affecting the characteristics of a material is the interphase layer structure. Previously,[3] it was shown that during the manufacture of a thermoplastic elastomer, an oil introduced into EPDM not only considerably improved its rheological properties but also altered the structure of the interphase layer. However, in this instance, the vulcanization of the rubber phase was simultaneously observed.

In this work, we selected EPR as the subject of study to eliminate the crosslinking effect during mixing. Moreover, due to the absence of unsaturated units in the chain, these copolymers possess high thermal stability, oxygen and ozone resistance, and photostability and show high resistance to aging and aggressive environments.

EXPERIMENTAL

In this study, we used iPP [weight-average molecular weight = 3.5×10^5, number-average molecular weight = 7.7×10^4, crystallinity = 55%, melting temperature (T_m) = 165°C] and the EPDMs Dutral CO 043 (EPR_{043}; propylene content = 45%, Mooney viscosity at 125°C = 34, oil-free) and Dutral CO 554 (EPR_{554}; propylene content =46%, Mooney viscosity at 125°C = 18, oil content = 50 wt %). The elastomeric specimens were kindly provided by Enichem Elastomeri (Milan, Italy).

iPP/EPR_{043} and iPP/EPR_{554} blends with rubber-phase contents varying from 0 to 100 wt % were prepared in a Brabender mixer at 180°C and a rotor speed of 100 rpm for 10 min. During the mixture of the polymers, torque on the mixer rotor was measured. The torque reached a limiting value of about 0.8 of its initial magnitude within 10 min, after which the mixing was ceased.

Correspondence to: A. O. Baranov (barand@polymer. chph. ras.ru).

Journal of Applied Polymer Science, Vol. 89, 249–257 (2003)

To examine the influence of oil and to accurately compare the morphology and mechanical properties of both types of rubber blends, we made the ratio of the base components (κ; iPP/elastomer per se, regardless of the oil content) identical for both systems. Blends with indices of κ = 4, 1, 0.5, and 0.25 were prepared.

From these blend compositions, samples were obtained as 1 mm thick plates by molding at 180°C under a pressure of 10 MPa followed by pressure cooling at a rate of about 30°C/min.

Rheological measurements were performed with an Instron capillary rheometer. The apparent viscosity (η_{app}) was calculated with the conventional procedure[4] by the following equation:

$$\eta_{app} = \tau_w / \dot{\gamma}_w$$

where

$$\tau_w = 3.51 \cdot 10^7 F d_c / L$$

is the shear stress on the capillary wall (F is the force with which the plunger presses on the polymer melt, d_c is the capillary diameter, and L is the capillary length);

$$\dot{\gamma}_w = \frac{2}{15} \frac{3n+1}{4n} V_p \frac{FD}{L}$$

is the shear rate on the capillary wall; n is the slope of $\ln \tau_w - \ln V_p$ dependence; V_p is the plunger velocity; and D is the cylinder diameter of the rheometer.

Thermophysical characteristics were determined by differential scanning calorimetry (DSC) with a Mettler TA 4000 instrument over a temperature range from −100 to 200°C in heating and cooling modes at a rate of 10°C/min.

The morphology of the obtained blends was studied with a Jeol JSM-35C scanning electron microscope. Samples for scanning electron microscopy (SEM) were prepared by low-temperature fracture and extraction of the rubber phase from a blend with *n*-heptane.

Mechanical measurements were carried out with an Instron 1122 testing machine at elongation rates V_e (speed of the upper grip) of 1, 5, 20, 50, or 100 mm/min at temperatures of 20, 60, and 100°C. Dumbbell specimens designed for testing had a working length (l_0) of 8 mm; the initial true strain rates ($V_\epsilon = V_e/l_0$) were 2.1×10^{-3}, 1.0×10^{-2}, 4.2×10^{-2}, 1.0×10^{-1}, and 2.1×10^{-1} s^{-1}, respectively. Five specimens were tested at each rate. The stress (σ) was calculated on the basis of the original cross-section of a sample. The elastic modulus (E) was determined from the initial slope of the stress–strain curves.

RESULTS AND DISCUSSION

Structure

The structure of polymer blends is defined to a considerable extent by the mixing conditions. Fine and uniform dispersion is achieved if the melt viscosities of components are close.[5,6]

A change in the relation between the viscosities of phase components depends on mixing temperature and $\dot{\gamma}_w$. Therefore, the viscosities of the initial polymer components were measured as a function of $\dot{\gamma}_w$ (Fig. 1). When $\dot{\gamma}_w$ was constant, the largest viscosity was observed for EPR_{043}, and the smallest viscosities were observed for iPP. The rubber-to-iPP viscosity ratio at $\dot{\gamma}_w$'s of greater than 150 s^{-1} varied within 2.7–3.0 and 1.2–1.5 for EPR_{043} and EPR_{554}, respectively. At $\dot{\gamma}_w \approx 1000$ s^{-1}, the viscosity values of for EPR_{554} and iPP differed insignificantly.

As shown in Figure 1, the blended polymers possessed viscosity values sufficiently close to one another under the experimental conditions in the temperature range 180–210°C and at $\dot{\gamma}_w$'s greater than 150 s^{-1}. Thus, good dispersion of the rubber in iPP could be expected, especially in the blends with an excess of iPP. This was indeed observed in the electron microscopic examination of the morphology, as shown in Figure 2. The dark areas represent the voids resulting

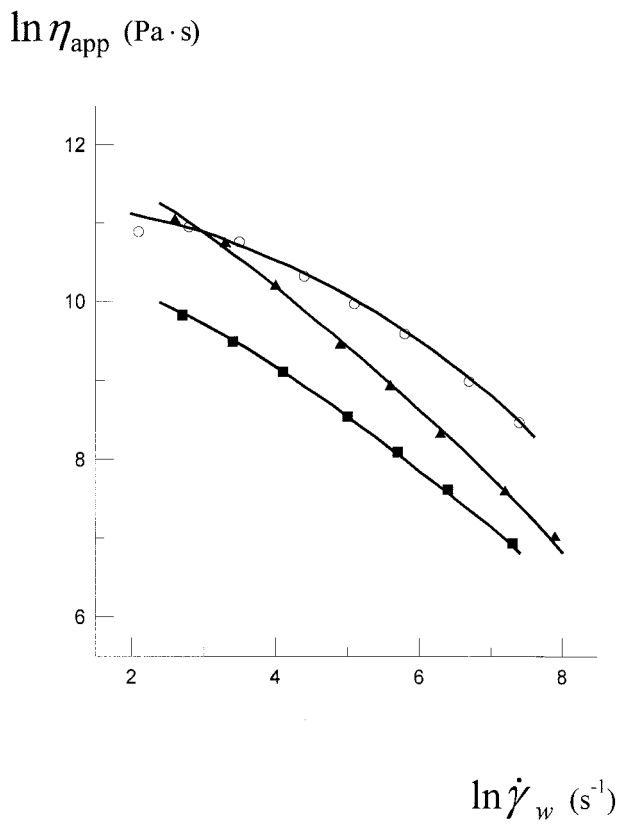

Figure 1 Dependency of the η_{app} of (■) iPP, (○) EPR_{043}, and (▲) EPR_{554} on $\dot{\gamma}_w$ at 200°C.

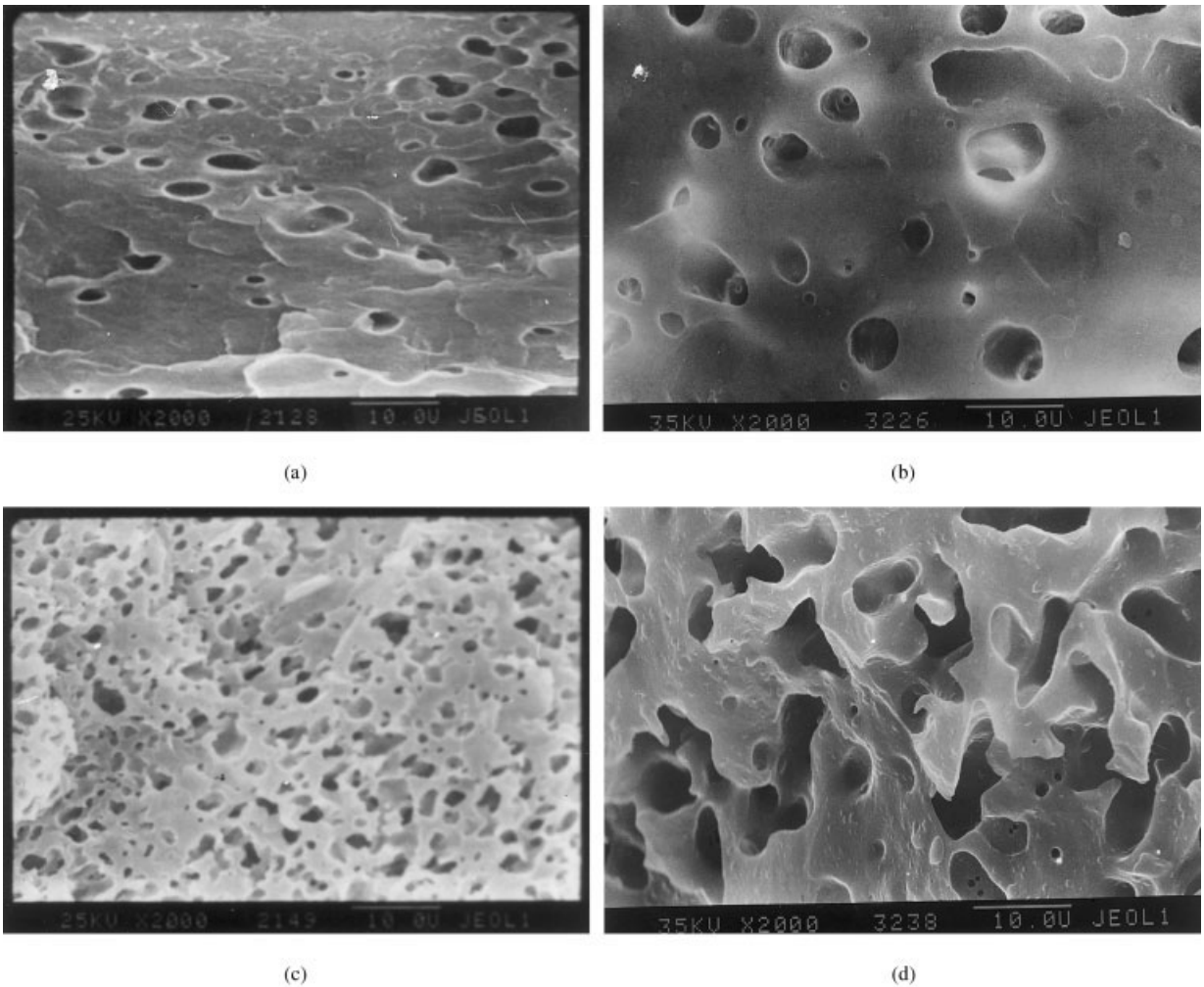

Figure 2 SEM micrographs of (a) 67/33 and (c) 20/80 iPP/EPR_{554} blends and (b) 80/20 and (d) 20/80 iPP/EPR_{043} blends. κ = (a,b) 4 and (c,d) 0.5. Magnification = 2000×.

from the solvent extraction of the rubber. Figure 2(a,b) shows that the blends with a prevalence of iPP ($\kappa = 4$) had a matrix structure, although the size and shape of the rubber particles in the iPP matrix depended on the presence of oil. The voids remaining after the extraction of EPR_{554} had an oval form, thus suggesting a lower viscosity of this oil-containing rubber and its higher compliance on shear blending with the thermoplastic [Fig. 2(a)].

Another picture was observed for blends with an excess of the elastomer [$\kappa = 0.5$; Figs. 2(c,d)]. Despite the fact that the interpenetrating network morphology[7] arose in both cases, the presence of oil substantially affected the component distribution pattern. As shown in Figure 2(c), EPR_{554} was uniformly dispersed with a particle size of the order of a few micrometers. The viscosity of EPR_{043} was much higher than that of EPR_{554} because of the absence of the oil. This considerably deteriorated the dispersion quality on blending with iPP. The size of rubber particles increased up to 10 μm, and their shape became irregular.

Thermophysical studies

As shown by the calorimetric studies in the heating and cooling modes, in the DSC curves of virgin components single peaks were observed; a narrow peak was observed for iPP, and broad peaks were observed for the elastomers both under heating and under cooling. For both types of EPR, the location of an endothermic peak under heating (near −10 to −20°C) and exothermic ones under cooling (near −20 to −30°C) and the corresponding areas under the DSC curves (enthalpy ΔH = 7–10 J/g) were reproduced considerably well in several heating–cooling cycles when errors in measuring the peak width and in the baseline construction were considered. However, the essence of this peak was not clear and requires further investigation, which was not the purpose of this work.

The glass-transition temperatures for EPRs of both types and for their blends were the same and ranged from −60 to −65°C. Another situation was observed for the T_m's and heats of melting (ΔH_m's) and crystal-

TABLE I.
T_m, ΔH_m, T_{cr}, and ΔH_{cr} of iPP in iPP/EPR$_{043}$ and iPP/EPR$_{554}$ Blends

Blend composition iPP/EPR/oil (wt %)	κ	T_m (K)	ΔH_m (J/g)	T_c (K)	ΔH_c (J/g)
iPP/EPR$_{043}$/oil					
100/0/0	—	438	80.0	384	86.9
80/20/0	4	438	84.8	383	82.8
50/50/0	1	438	82.0	383	86.0
20/80/0	0.25	433	70.0	373 (317)	62.5 (8.3)
iPP/EPR$_{554}$/oil					
100/0/0	—	438	80.0	384	86.9
66.70/16.65/16.65	4	432	80.6	379	85.2
20.00/40.00/40.00	0.5	428	86.5	373	86.5
11.10/44.45/44.45	0.25	426	76.6	354 (309)	74.2 (5.2)

lization temperatures (T_c's) and heats of crystallization (ΔH_c's) of iPP (see Table I). For EPR$_{043}$ blends with an iPP content of $w_{iPP} \geq 50$ wt %, these parameters remained almost unchanged and decreased only with an excess of EPR. A similar effect for T_m has been already reported.[8,9]

The influence of the amorphous component of the blend on T_m of a crystalline polymer can be analyzed on the basis of the Nishi–Wang equation:[10]

$$\frac{T_m}{T_m^*} = 1 + B\,\frac{\nu_2}{\Delta H_m^*}\,\varphi_2^2. \qquad (1)$$

where $B = \chi_{12}RT/\nu_2$ at $T = T_m$; T_m^* is the melting temperature of pure iPP measured under the same heating conditions as for the blends; ν_2 is the molar volume of oil-extended EPR; ΔH_m^* is the standard enthalpy of melting of iPP; χ_{12} is the compatibility parameter; ϕ_2 is the volume fraction of EPR in a blend; and R is the gas constant.

Equation (1) corresponds to thermodynamic equilibrium T_m's, which are determined by a rather laborious extrapolation procedure.[11] In this work, we measured T_m under the same scanning conditions without determination of the equilibrium T_m values. The plot of T_m as a function of ϕ_2^2, calculated according to the eq. (1), is given in Figure 3. Although this plot is qualitative in character, it can be seen that a change in T_m/T_m^* was indeed described by eq. (1). The parameter B and, hence, χ_{12} were negative. This is an indication of the somewhat limited compatibility of EPR$_{554}$ with iPP. Most probably, on blending the components in a melt, oil-extended EPR dissolved some amount of the iPP molecules with low molecular weight and/or with more imperfect structure. This must have resulted in the formation of an interphase layer enriched in rubber and iPP molecules and affected the properties of the blend.

The presence of oil-extended EPR in the blend must also have affected the crystallization of iPP. Indeed, T_c linearly decreased with increasing EPR$_{554}$ content, first decreasing linearly and then drastically dropping. With an excess of EPR of any type in a blend, the DSC cooling curves exhibited two crystallization peaks. It is likely that low-temperature and high-temperature iPP phases were formed in this case.

These results were supported by the analysis of crystallization rate curves. The weight fraction of crystallized polymer at a given time was determined in the conventional manner.[12] The crystallization rate dramatically decreased at a high elastomer content, regardless of the presence of oil. At the same time, at iPP contents of greater than 50 wt % in the iPP/EPR$_{043}$ blends, the rubber did not affect the crystallization

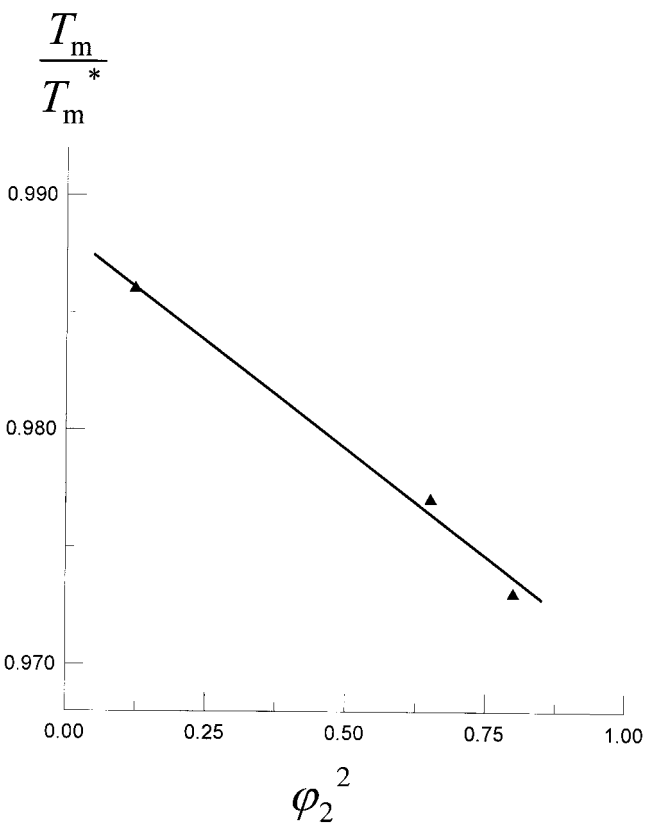

Figure 3 Relative melting temperature T_m/T_m^* of iPP as a function of ϕ_2^2, the squared volume fraction of EPR$_{554}$.

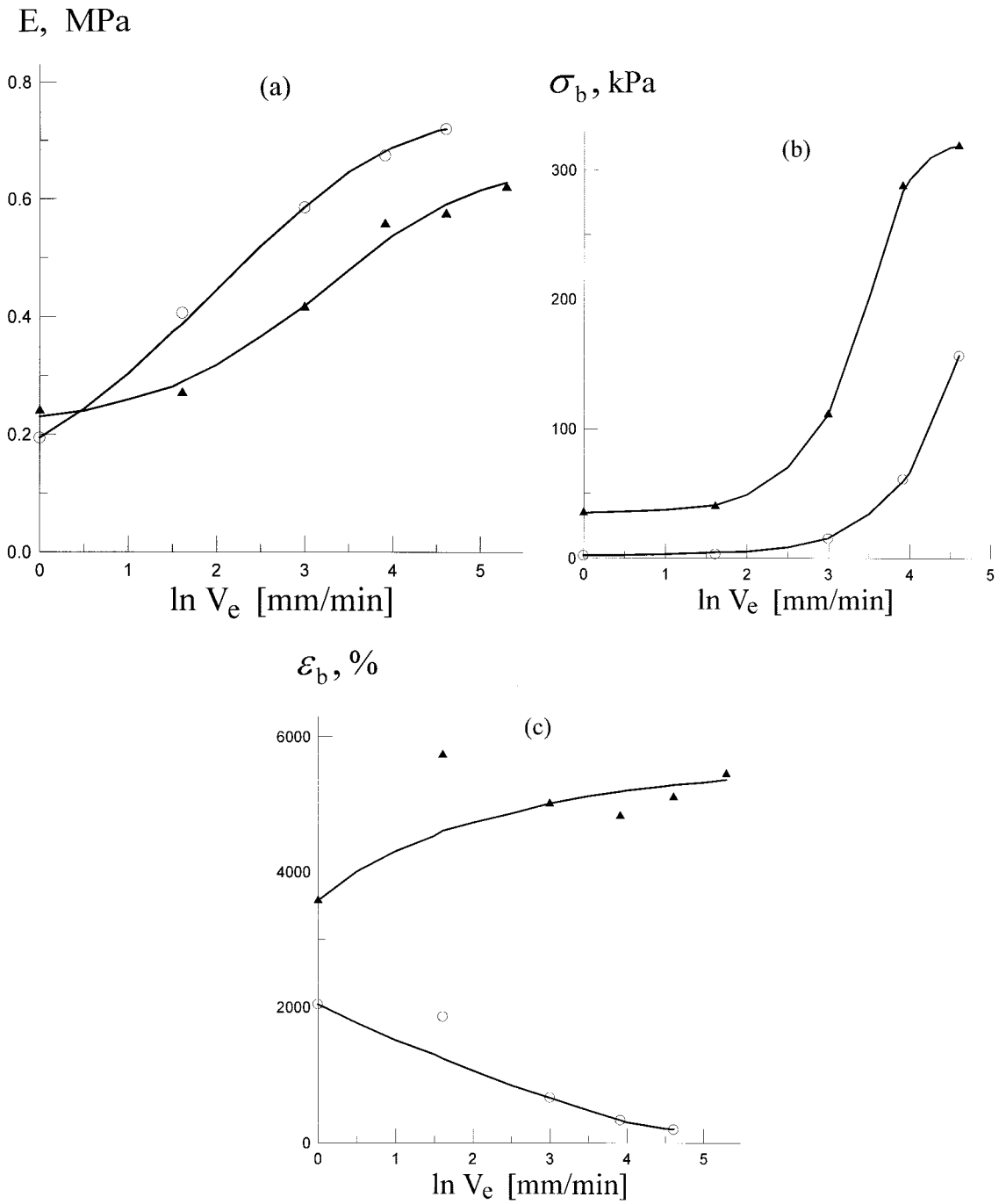

Figure 4 Plots of (a) E, (b) σ_b, and (c) ϵ_b for (○) EPR_{043} and (▲) EPR_{554} versus ln V_e at 20°C.

kinetics. In the presence of oil in the iPP/EPR_{554} blends, the induction period decreased with increasing rubber content, and the iPP crystallization rate was independent of the amount of the second component. Probably, the molecules of the second component (rubber–oil) acted as iPP crystallization nuclei in this case. It could be assumed that the extraction of iPP macromolecules and the formation of the iPP–EPR interphase layer took place on the blending of iPP with oil-containing EPR.

Mechanical properties of the elastomers

The presence of oil in the rubber and in the blend affected not only the thermophysical but also the mechanical properties of the material. The mechanical properties under tension of virgin iPP are quite typical.[13] The stress–strain diagrams showed a typical semicrystalline polymer appearance when the iPP samples formed the neck. The dependencies of E, ultimate tensile strength (σ_b), and elongation at break

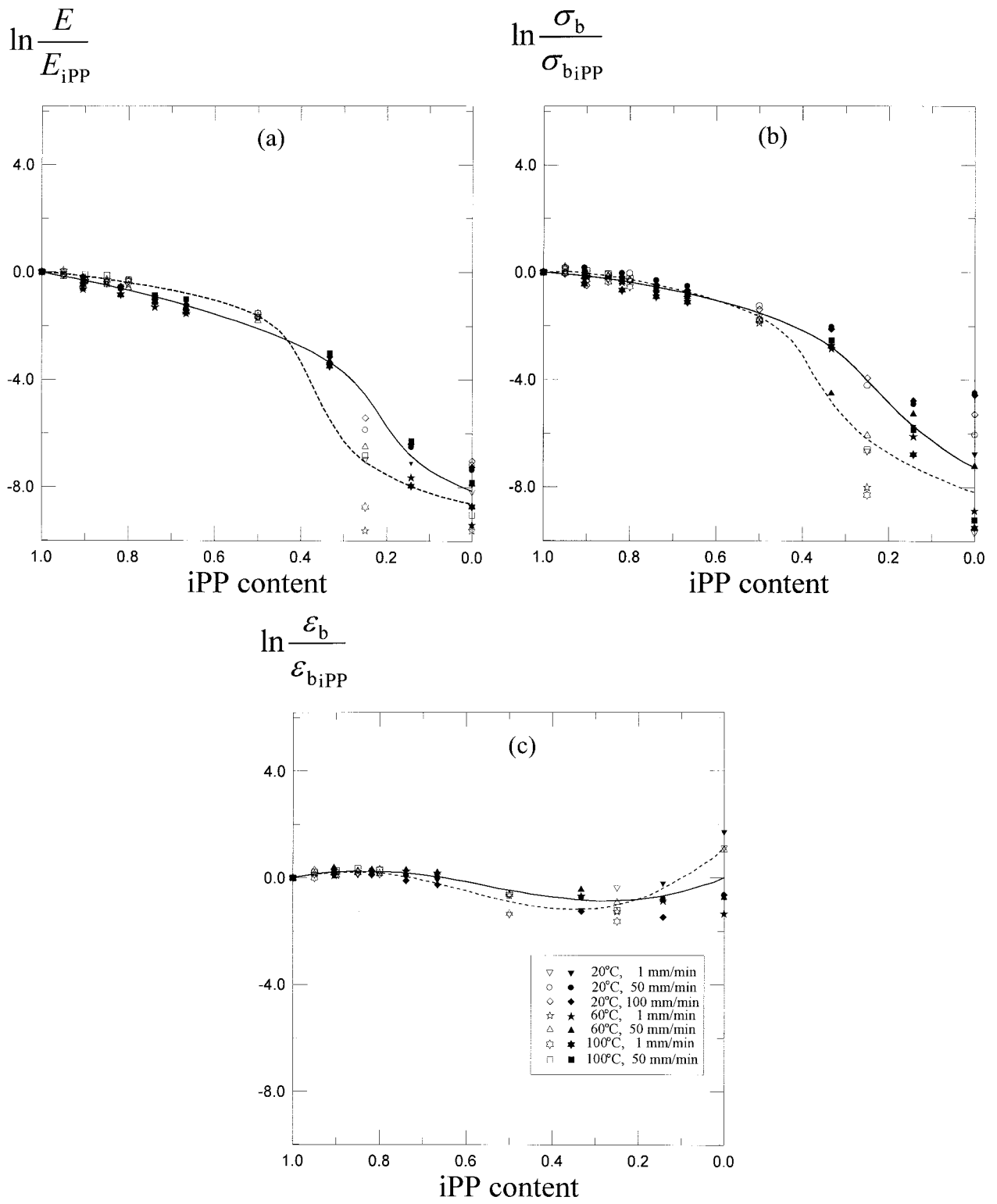

Figure 5 Plots of the reduced properties (a) E/E_{iPP}, (b) $\sigma_b/\sigma_{b\ iPP}$, and (c) $\epsilon_b/\epsilon_{b\ iPP}$ for iPP/EPR_{043} (light symbols) and iPP/EPR_{554} (dark symbols) blends versus the iPP content. The curves depicts average data for (– –) iPP/EPR_{043} and (—) iPP/EPR_{554} blends.

(ϵ_b) on temperature and V_e were similar to the dependencies represented in refs. 13 and 14.

The stress–strain diagrams for both elastomer types were also quite typical of amorphous polymers. The E's of EPR_{043} and EPR_{554} increased with increasing V_e, with the E values for EPR_{554} being lower than those for EPR_{043}, except at V_e = 1 mm/min [Fig. 4(a)].

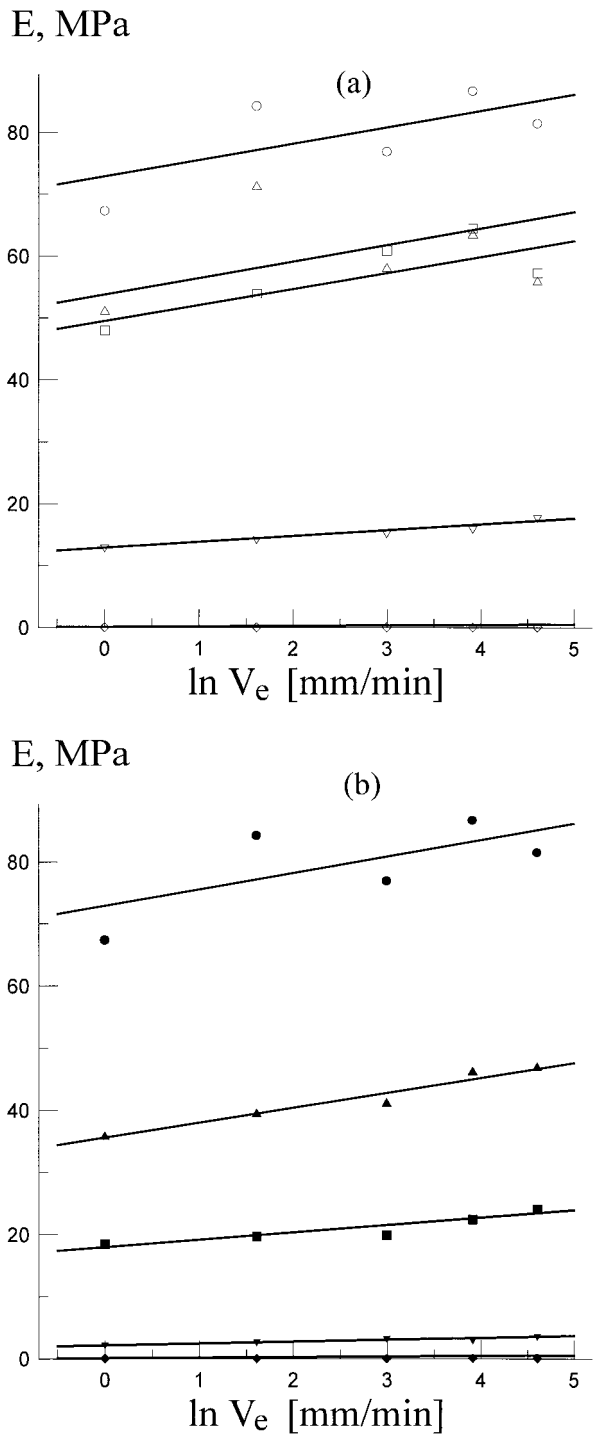

Figure 6 Dependencies of E on ln V_e for (a) iPP/EPR$_{043}$ and (b) iPP/EPR$_{554}$ blends at iPP/EPR$_{043}$ = (○) 100/0, (△) 90/10, (□) 80/20, (▽) 50/50, and (◇) 0/100 and iPP/EPR$_{554}$ = (●) 100/0, (▲) 81.8/18.2, (■) 66.7/33.3, (▼) 33.3/66.7, and (◆) 0/100.

Because EPR$_{554}$ contained the oil, which bore no mechanical load, it was necessary to consider a fraction of the elastomer in the estimation of the cross-section and σ for low deformation values. ν_0 and ν are the molar volumes of EPR without oil and of oil-extended EPR, respectively (hereinafter the subscript "0" refers to oil-free elastomer). Then, $\xi = \nu_0/\nu$ is the volume fraction of elastomer. As a result, we obtain:

$$\sigma_0 = \frac{f}{S_0} = \frac{f}{\nu_0^{2/3}}$$

for EPR$_{043}$ and

$$\sigma = \frac{f}{S} = \frac{f}{\nu^{2/3}} = \frac{f}{\nu_0^{2/3}}\,\xi^{2/3} = \sigma_0\,\xi^{2/3}$$

for EPR$_{554}$, where f is the tensile force. The experimental results indicated that the E/E_0 value changed in the range 0.7–0.8. This value was satisfactorily consistent with the calculated value of 0.65. Therefore, in the evaluation of E of oil-containing rubbers, it is necessary to consider the presence of the oil, which sustains no mechanical load. At large deformations, σ_b of EPR$_{554}$ exceeded σ_b of EPR$_{043}$ at all V_e values [Fig. 4(b)]. For EPRs of both types, σ_b changed in a similar manner, depending on ln V_e.

Another situation was observed for the dependency of ϵ_b on V_e [Fig. 4(c)]. As shown, for EPR$_{043}$ ϵ_b decreased by almost an order of magnitude with increasing V_e. At the same time, ϵ_b increased with increasing V_e for the oil-extended elastomer EPR$_{554}$. It could be supposed that such a characteristic of changing the σ_b and ϵ_b values with V_e was determined by both the molecular structure

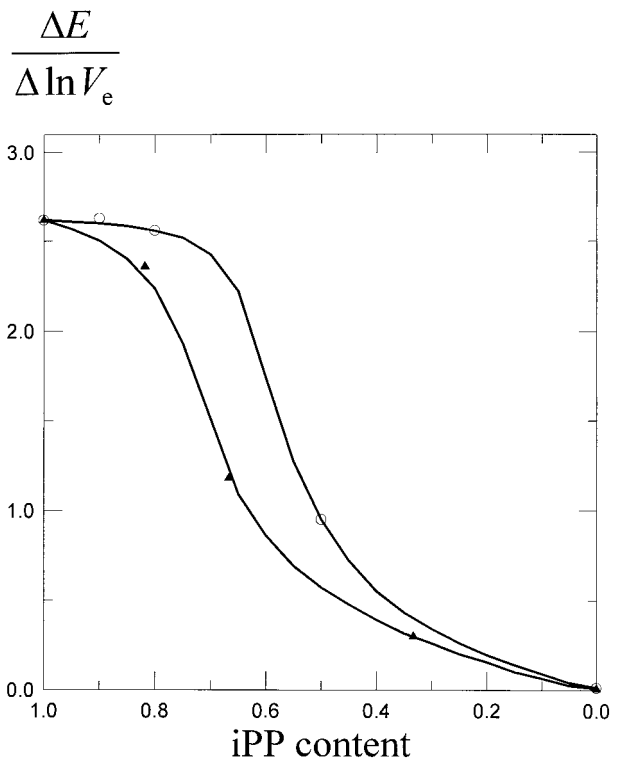

Figure 7 Plots of $\Delta E/\Delta$ ln V_e versus the iPP content for (○) iPP/EPR$_{043}$ and (▲) iPP/EPR$_{554}$ blends.

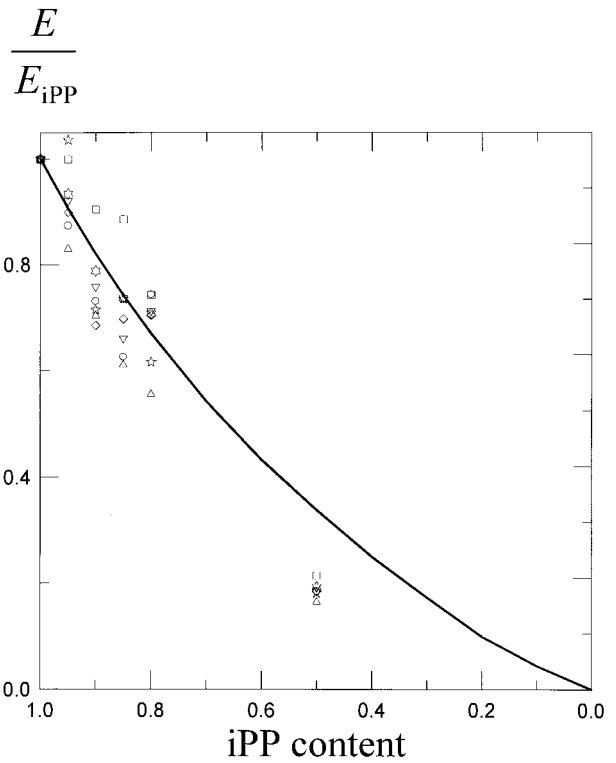

Figure 8 Dependencies of E on the iPP content for the iPP/EPR$_{043}$ blend. The curve represents values calculated with the Kerner equation. The notation of data points is the same as in Figure 5.

of EPR and the presence of oil. To separate these factors, it will be necessary to later study the influence of oil content for EPR of the same type.

Nevertheless, the observed dependence of ϵ_b on V_e could be explained in terms of the following model. ϵ_b as a function of V_e had a maximum that was due to relaxation processes.[15,16] Much more likely was that when the oil was added to the elastomer, its relaxation spectrum changed. Then, ϵ_b decreased for EPR$_{043}$; however, it increased for EPR$_{554}$ with increasing V_e over the examined V_e range; that is, the compared spectra corresponded to different positions of the $\epsilon_b(V_e)$ curves with respect to the maximum.

Mechanical properties of blends

Figure 5 presents E, σ_b, and ϵ_b data plotted against the iPP content. The values of E and σ_b decreased to a relatively small extent with decreasing iPP content down to about 50 wt % but dramatically dropped on any further decrease in the iPP content. This was most probably due to phase inversion [Fig. 2(c)]. At the same time, ϵ_b varied insignificantly with decreasing iPP content.

Figure 6 depicts plots of E versus ln V_e. As shown, the slope of the straight lines decreased with increasing rubber content, and for the virgin elastomers, E was almost independent of V_e. For the oil-free blend with the prevalence of iPP, the slope was constant, but it dramatically decreased on phase inversion. However, for the oil-containing blends, a drop in E was

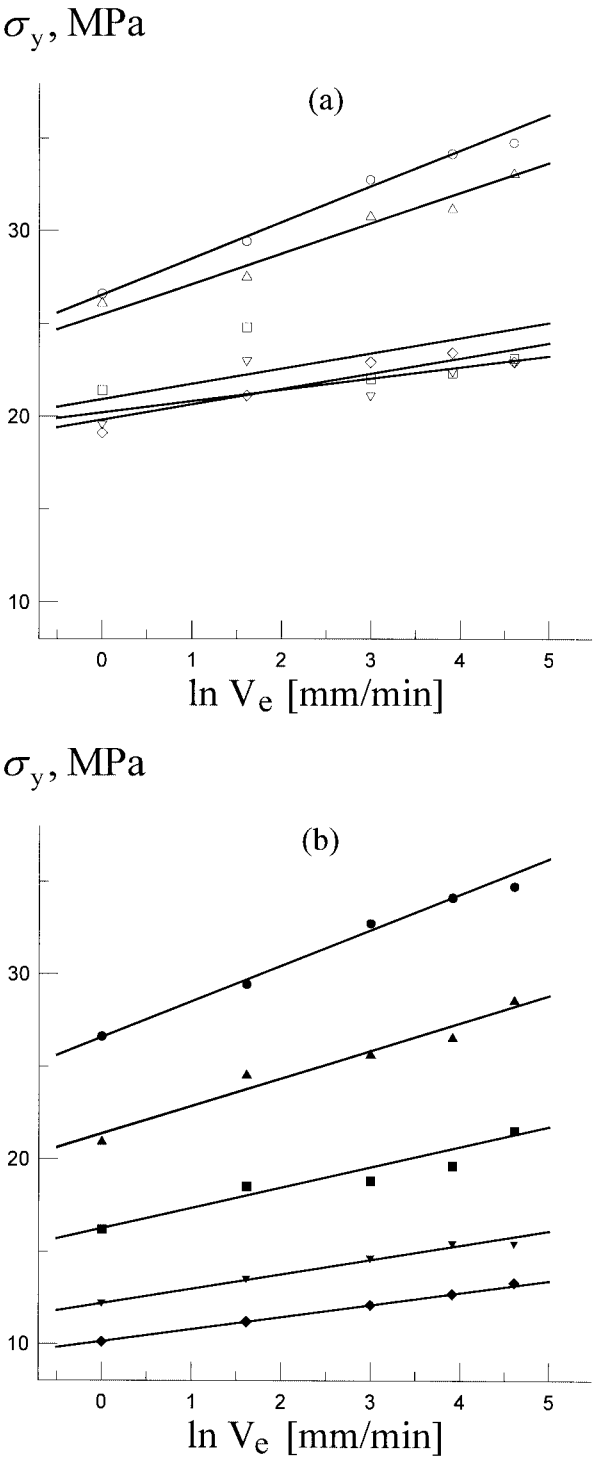

Figure 9 Tensile σ_y as a function of ln V_e for (a) iPP/EPR$_{043}$ and (b) iPP/EPR$_{554}$ blends at iPP/EPR$_{043}$ = (○) 100/0, (△) 95/5, (□) 90/10, (▽) 85/15, and (◇) 80/20 and iPP/EPR$_{554}$ = (●) 100/0, (▲) 90.5/9.5, (■) 81.8/18.2, (▼) 73.9/26.1, and (◆) 66.7/33.3.

TABLE II
γ Depending on the Blend Composition

iPP/EPR_{043}	$\gamma \times 10^3$ (m^3/mol)	iPP/EPR_{554}	$\gamma \times 10^3$ (m^3/mol)
100/0	1.60	100/0	1.60
95/5	1.60	90.5/9.5	1.53
90/10	1.87	81.8/18.2	2.40
80/20	2.24	66.7/33.3	3.35

observed even with a small decrease in iPP content (Fig. 7).

Figure 8 shows the plot of E as a function of iPP content up to 70 wt % for the iPP/EPR_{043} blend. A quantitative estimate for the modulus E was obtained with the Kerner equation:[17]

$$\frac{E}{E_{iPP}} = \frac{1}{1 + \dfrac{15(1 - \mu_{iPP})(1 - \varphi_{iPP})}{(7 - 5\mu_{iPP})\varphi_{iPP}}}$$

where μ_{iPP} is the Poisson ratio for iPP and ϕ_{iPP} is the volume fraction of iPP in the blend. This model satisfactorily described the experimental values of E only at low iPP contents. At low iPP contents, the calculated values of E exceeded the experimental ones, and the differences increased with increasing elastomer content. This was probably due to change in blend structure.

A similar theoretical estimation of the concentration dependency of E for iPP/EPR_{554} blend was rather difficult because of the presence of the oil.

The stress–strain diagrams for blends with a prevalence of iPP displayed the yield points at the yield stress (σ_y). Figure 9 shows the dependence of σ_y on ln V_e for iPP blends with different EPR brands. The experimental results were described well with a linear relationship, wherein the slope and E decreased with increasing rubber content. The dependence of σ_y on ln V_e is described by the Eyring equation:[18]

$$\sigma_y = \frac{U}{\gamma} + \frac{RT}{\gamma} \ln \frac{V_e}{V_{e0}},$$

where R is the gas constant, T is the absolute temperature, V_{e0} is the standard deformation rate, U is the activation energy, and γ is the activation volume. The experimentally determined γ's are listed in Table II. The value of γ increased with increasing rubber content. For the oil-extended rubber, γ increased more strongly than for the oil-free elastomer. This was obviously due to the fact that the oil facilitated the plastic flow process by changing the relaxation spectrum.[16] Thus, the introduction of oil into elastomer resulted in an increase in the compatibility of the elastomer with iPP in consequence of the interphase layer formation, increasing the γ on deformation and modifying the plastic flow process.

CONCLUSIONS

We conclude that the use of oil-extended elastomer (EPR_{554}) in iPP/EPR blends resulted in structural changes in the interphase layer during the component blending. It seemed that the oil-containing EPR_{554} dissolved some of the iPP molecules with low molecular weights and/or more imperfect structures.

According to the Eyring equation, we calculated γ's from the dependencies of σ_y of the iPP/EPR blends on the logarithm of V_e. It was experimentally demonstrated that the γ values increased with increasing rubber content; moreover, for the oil-containing rubber EPR_{554}, this increase in γ was more pronounced than for the oil-free elastomer EPR_{043}. Consequently, the σ_y value was less dependent V_e.

The ultimate ϵ_b increased for the oil-containing EPR_{554} but decreased for EPR_{043} with increasing V_e. However, further studies are required because it is not known whether or not this is a common phenomenon for all polymer–rubber blends.

References

1. Polypropylene: Structure, Blends and Composites; Karger-Kocsis, J., Ed.; Chapman & Hall: London, 1995; Vol. 2.
2. Polypropylene Handbook; Moore, E. P., Jr., Ed.; Hanser: Munich, Germany, 1996.
3. Prut, E. V. In Proceedings of the IV Session of the International School of Chemical Engineering Science for Advanced Technologies; Karpov Institute of Physical Chemistry: Moscow, 1998; p 94.
4. Malkin, A. Y.; Chalykh, A. E. Diffusion and Viscosity of Polymers: Measurement Techniques; Khimiya: Moscow, 1979.
5. Kuleznev, V. N. Polymer Blends; Khimiya: Moscow, 1980.
6. Baranov, A. O.; Medintseva, T. I.; Zhorina, L. A.; Zelenetskii, A. N.; Prut, E. V. J Appl Polym Sci 1999, 73, 1563.
7. Manson, J. A.; Sperling, L. H. Polymer Blends and Composites; Plenum: New York, 1976.
8. Karger-Kocsis, J.; Kalló, A.; Szafner, A.; Bodor, G.; Sényei, Z. Polymer 1979, 20, 37.
9. Martuscelli, E.; Silvestre, C.; Bianchi, L. Polymer 1983, 24, 1458.
10. Nishi., T.; Wang, T. T. Macromolecules 1975, 8, 909.
11. Hoffman, Y. D.; Weeks, J. J. J Res Natl Bur Stand A 1962, 66, 13.
12. Bershtein, V. A.; Egorov, V. M. Differential Scanning Calorimetry in Physical Chemistry of Polymers; Khimiya: Leningrad, 1990.
13. Erina, N. A.; Knunyants, M. I.; Dorfman, I. Y.; Kryuchkov, A. N.; Prut, E. V.; Enikolopyan, N. S. Dokl Akad Nauk 1985, 280, 913.
14. Springer, H.; Schenk, W.; Hinrichsen, G. Colloid Polym Sci 1983, 261, 9.
15. Fracture; Liebowitz, H., Ed.; Academic: New York, 1972; Vol. 7, Chapter II.
16. Bartenev, G. M. Structure and Relaxation Properties of Polymers and Composites; Khimiya: Moscow, 1979.
17. Nielsen, L. E. Mechanical Properties of Polymers and Composites; Marcel Dekker: New York, 1974.
18. Krausz, A. S.; Eyring, H. Deformation Kinetics; Wiley: New York, 1975.